Peer-reviewed version available at *Water* **2018**, *10*, 1045; doi:10.3390/w10081045

Clogging Impacts on Distribution Pipe Delivery of Street Runoff to an Infiltration Bed

Min-Cheng Tu[1], Ph.D.

Robert G. Traver[2], Ph.D., P.E., D. WRE

[1] Postdoctoral Research Fellow, Department of Civil and Environmental Engineering, Villanova University, Villanova, PA 19085 (corresponding author). Email: min-cheng.tu@villanova.edu

[2] Professor, Department of Civil and Environmental Engineering, Villanova University, Villanova, PA 19085. Email: robert.traver@villanova.edu

Abstract

Performance of flow through orifices on a perforated distribution pipe between periods with and without partial clogging (submersion of part of the distribution pipe) was compared. The distribution pipe directly receives runoff and delivers it to an underground infiltration bed. Partial clogging appeared in winter but reduced in summer. Performance was defined as flow rate divided by $l_{eff}\sqrt{h_{d,mean}}$ where $h_{d,mean}$ is the mean pressure head that drives flow and l_{eff} is the effective pipe length (length of water column with pipe water volume and the pipe cross-sectional area). ANCOVA (ANalysis of COVAriance) was adopted to examine the clogging effects with flow rate plotted against $l_{eff}\sqrt{h_{d,mean}}$. Partial clogging had a significant effect on pipe performance during periods of low or no rainfall. However, if only data during larger storms was considered, little evidence showed that partial clogging had effects on pipe delivery performance. Partial clogging might be caused by leaves accumulated in the lower section of the pipe in winter, and its effect was insignificant when water level rose in the pipe, utilizing significantly more orifices on the distribution pipe, thus the effect from the clogged portion had negligible impact on system performance. Larger storms might also provide the required flow rate to move the debris block thus exposing the orifices. Partial clogging did not increase the tendency of overflow; therefore, current maintenance schedule was sufficient to keep the distribution pipe at satisfactory performance even though partial clogging can exist.

Key Words

ANCOVA; Blockage; Clogging; Efficient; Green infrastructure; Infiltration bed; Orifice; Perforation; Performance; Philadelphia; Pipe; Stormwater

Introduction

The use of underdrain distribution pipes in the design of Stormwater Control Measure (SCM) is a common practice in bioretention and permeable pavement systems, particularly when the subsoils have lower infiltration properties [1]. These underdrains are designed to evacuate water from a SCM to a defined outfall point. Most analyses for clogging of such systems are limited to clogging of the filtering media [2-4] or the permeable pavement surface [5-6], with a few studies focusing on clogging of distribution pipes under permeable pavement systems [7]. Since sediment is primarily captured by the surface layer [8], clogging of distribution pipes are not considered by most studies, and distribution pipes are considered not a restriction to water movement [9].

In Philadelphia, the "Green City, Clean Waters" initiative was adopted in 2011 as part of the city's Combined Sewer Overflow Long Term Control Plan. Over 1,100 green infrastructures (GIs) have been built in Philadelphia since then [10]. Due to the limited building space in Philadelphia, many of the GIs are built under sidewalks in the road right-of-way. For a typical tree trench GI built in Philadelphia, runoff from the road surface enters an inlet structure, and a perforated distribution pipe transports and delivers water into the subsurface infiltration bed (i.e. a SCM), thus the flow direction is reversed from that of the application described earlier. Pretreatement is limited to a trash guard (a meshed filter bag) under the inlet grate or a sumped inlet due to space constraints.

Clogging analyses for similar systems are scarce. Hydraulic performance of similar systems has been investigated [11-12], but not the effects and characteristics of clogging of an inflow distribution pipe as far as the authors can find. From the related field of drip irrigation, past studies indicate that clogging is possible in similar systems [13], but the differences in pipe specifications and sources of water preclude direct comparison. **Error! Reference source not found.** In addition to sediment, trash and/or leaves, stormwater runoff from road surfaces can be products from vehicle waste, atmospheric deposition, and road materials [14]. Since the characteristics of non-point pollution from stormwater runoff are complex [15], studies dedicating to clogging of distribution pipes from untreated stormwater runoff are required.

Urbanization is a global trend. More than 50% of world population have moved into urban areas by 2010, and such population shift had been achieved in the United States in the early 20th century [16]. As urban area expands, controlling non-point pollution from urban areas becomes more important. For such urban areas with limited building space, designs similar to the tree trench GI**Error! Reference source not found.** built in Philadelphia will play an important role in the future of urban stormwater management. Therefore, it is essential to understand the effects and characteristics of clogging and a cost-effective strategy in maintenance of distribution pipes of such systems.

Site Information

The SCM under investigation was constructed in 2013 in the northern suburban area of Philadelphia, Pennsylvania at approximately 40.07°N, 75.17°W (the sidewalk outside Hill Freedman World Academy). It is in the Cfa (humid subtropical) climate region according to the Koppen-Geiger climate classification system [17] with an average annual precipitation of 1,054 mm from 1981 to 2010 [18]. Most monthly

Preprints (www.preprints.org) | NOT PEER-REVIEWED | Posted: 4 July 2018 doi:10.20944/preprints201807.0075.v1

Peer-reviewed version available at Water 2018, 10, 1045; doi:10.3390/w10081045

precipitation is distributed from 76 mm to 97 mm, with the exceptions of February as the driest month (66 mm) and July as the wettest month (109 mm). The average annual snowfall is 584 mm, typically from December to April with a peak in February.

As shown in *Figure 1*, this system is composed of five curbside planters, an underground rock infiltration bed in which the planters sit, two inlet structures (GI1 and GI2) collecting runoff from both sides of the street (with directly connected impervious drainage area of 2,494 m^2), and one distribution pipe delivering water collected by the inlet structures to the rock infiltration bed. The two inlet structures (GI1 and GI2 in the top section of *Figure 1*) are connected by a culvert with a diameter of 203.2 mm (sloped to GI1). Another perforated pipe with the same diameter (sloped to GI1) delivers water from the GI1 curb inlet structure to the rock bed (bottom section of *Figure 1*). Meshed trash guards (*Figure 2*) are installed in each inlet structure to reduce the amount of trash entering the distribution pipe. Inside the rock bed, the distribution pipe is uniformly perforated with unspecified specification (personal communication with Philadelphia Water Department) and has an adverse 0.5% slope following the general design practice to bring debris towards the pipe entrance by gravity to facilitate maintenance cleaning. The only overflow points of the system are the street inlets GI1 and GI2, with GI1 located at a lower elevation. All dimensions are based on design drawings and post-construction invert measurements.

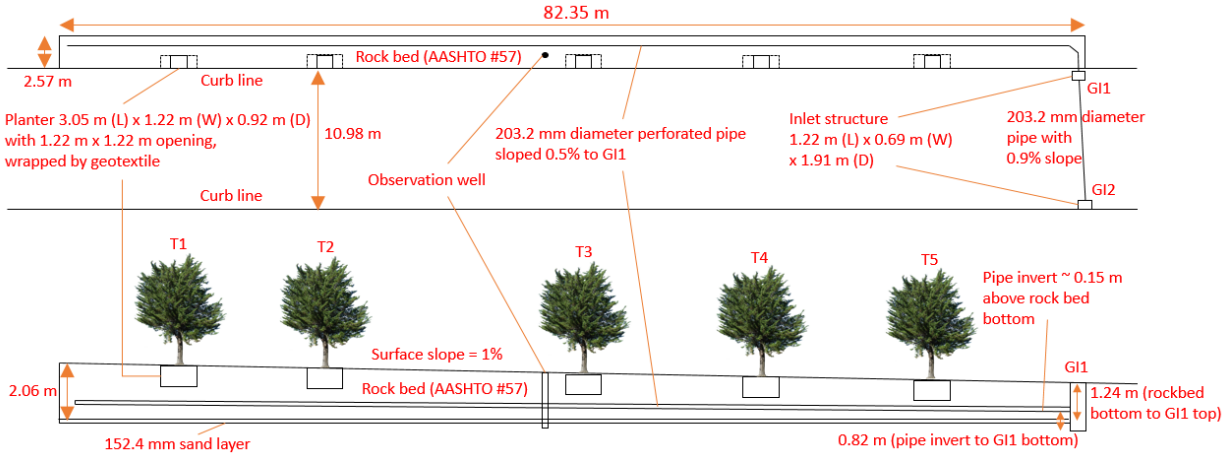

Figure 1. Plan view (top) and profile view (bottom) of the site under investigation

Preprints (www.preprints.org) | NOT PEER-REVIEWED | Posted: 4 July 2018 doi:10.20944/preprints201807.0075.v1

Peer-reviewed version available at *Water* **2018**, *10*, 1045; doi:10.3390/w10081045

Figure 2. Trash guard installed in GI1 inlet structure (Date: October 18, 2016).

Instrumentation for this site includes a weather station (comprised of a Campbell CR800 data logger, a LI200X-L pyranometer, a TE525 rain gage [19], a Hukseflux LP02-L25-P pyranometer [20] and a Vaisala WXT520 multi-purpose weather station [21]), one HOBO [22] pressure transducer in each inlet structure (two total), an area-velocity sensor with ProSiren data logger [23] to measure the flow rate entering the distribution pipe at the entrance, a HOBO pressure transducer at the bottom of an observation well in the the rock bed, and one set of soil moisture sensors [24] at various depths in each tree pit (five sets in total). All data has the same temporal interval of 5 minutes.

Observation

During the period from June 2016 to April 2018, periodic ponding in the inlet structure that submerged part of the distribution pipe entrance was observed during several field visits. Figure 3 shows a typical situation of such partial clogging. Collected water depth data of GI1 inlet structure provided a more holistic view for periods of such partial clogging in Figure 4. The overflow depth of the inlet structure and the invert of the distribution pipe inlet are marked with black horizontal lines in Figure 4.

Preprints (www.preprints.org) | NOT PEER-REVIEWED | Posted: 4 July 2018 doi:10.20944/preprints201807.0075.v1

Peer-reviewed version available at *Water* **2018**, *10*, 1045; doi:10.3390/w10081045

Figure 3. Ponding in the inlet structure due to partial clogging of the distribution pipe (Date: March 30, 2017)

Figure 4 shows several long episodes of partial clogging, as exhibited by continuous ponding above the invert of the pipe inlet (0.82 meter), during the following range of dates: Feb 25, 2017-Apr 10, 2017, Apr 17, 2017-May 5, 2017, and after Jan 31, 2018. Ponding was also observed before Jan 25, 2017, but data collection was interrupted in winter 2016-2017 so the beginning of that partial clogging episode cannot be determined. On Jan 25, 2017, a subsurface distribution pipe cleaning was performed, comprising injection of pressurized water jets into the distribution pipe and subsequent vacuuming. This is the only subsurface cleaning during the observation period from June 2016 to April 2018. Following the cleaning, the partial clogging situation was solved for a short period of time but reconstituted during the storm on Feb 25, 2017. Note that all long partial clogging episodes happened in winter or spring.

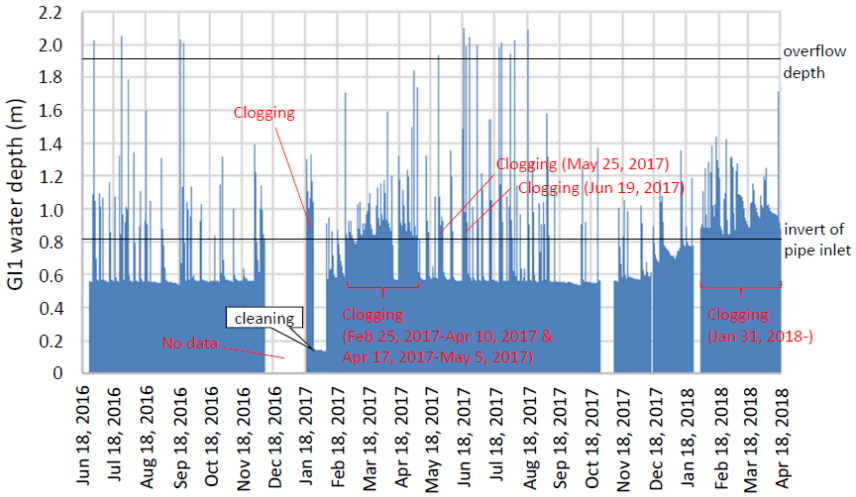

Figure 4. Water elevation in GI1 inlet structure between June 2016 and April 2018

In addition to those long episodes, several short episodes of partial clogging (e.g. May 25, 2017 and Jun 19, 2017) were also evident during summer. May 25, 2017 contained two events with the first event being free from and the second exhibiting significant partial clogging, as *Figure 5* shows. Rainfall

Preprints (www.preprints.org) | NOT PEER-REVIEWED | Posted: 4 July 2018 doi:10.20944/preprints201807.0075.v1

Peer-reviewed version available at Water 2018, 10, 1045; doi:10.3390/w10081045

associated with the two storms was separated by more than six hours, so they were considered two distinct storms. After the first peak of the second storm, water depth recession rate in the GI1 inlet structure after cessation of rainfall reduced significantly compared to that of the first storm, showing partial clogging of the distribution pipe. For all storms, water level in the rock bed is always lower than that in the inlet structure, as *Figure 5* shows. In *Figure 5*, the bottom of the inlet structure is the datum for all water depths or elevations. Because the bottom of rock bed is higher than that of inlet structure, water depth in the rock bed showed a flat line when dry.

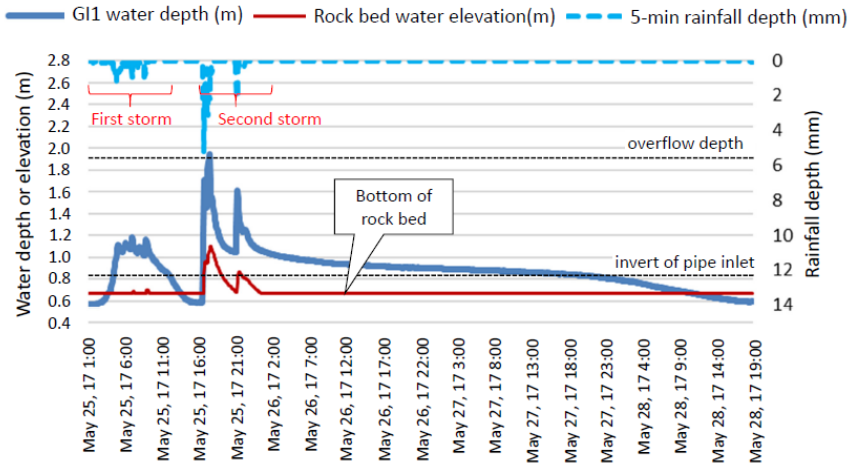

Figure 5. Rainfall depth and water depth (inlet structure and rock bed, with the bottom of inlet structure as datum) from events without (first storm) and with (second storm) partial clogging on May 25, 2017

One phenomenon that has not been explained in both Figure 4 and Figure 5 was the low water depth in the inlet structure at the final balance state for periods without partial clogging. It was at around 0.6 meter from the bottom and significantly lower than the invert of the distribution pipe inlet (0.82 meter), which can only be caused by a leaking inlet structure. The leaking rate varied significantly possibly because of the variation of soil moisture and groundwater level in the surrounding soil. For example, based on the water depth recession rate from the invert of the pipe inlet (0.82 meter) to the final depth (0.6 meter), Figure 5 shows a much faster leaking rate for the first storm than that for the second storm. Nevertheless, the leaking rate was very small at about 8e-6 m^3/s (based on the first storm of Figure 5) or less, so its effect can be ignored. Water recession is accelerated below the pipe invert in Figure 5 because the water surface area above the pipe invert (i.e. including water in the pipe) would be much larger than that between the invert of the pipe inlet and the leaking point (i.e. only water in the inlet structure). The leaking point in the inlet structure was located during the subsurface pipe cleaning on Jan 25, 2017 when the inlet structure was pumped dry, shown as the small stream of water circled by the red oval in *Figure 6*. In *Figure 6*, water flows back into the inlet structure possibly because the surrounding soil was saturated from the high ponding situation before Jan 25, 2017.

Preprints (www.preprints.org) | NOT PEER-REVIEWED | Posted: 4 July 2018 doi:10.20944/preprints201807.0075.v1

Peer-reviewed version available at Water 2018, 10, 1045; doi:10.3390/w10081045

Figure 6. Leaking point in the inlet structure (Date: January 25, 2017)

The observations based on field visits and collected data showed a complicated nature of partial clogging of the distribution pipe. Despite a few short episodes in summer, most partial clogging episodes were clustered in winter. The effect of undersurface pipe cleaning was short lived in winter, but most of the partial clogging situations mitigated by itself in summer without human intervention. Even though such partial clogging did not appear to increase the tendency of overflow (only the short episode on Jun 19, 2017 had overflow), how such partial clogging affected the performance of the distribution pipe should be understood. If an impact on the distribution pipe performance did exist, the patterns of its influence (i.e. uniform influence across all storms, or higher influence towards small/large storms) should be evaluated in order to decide the maintenance strategy against such partial clogging, and to avoid loss of system performance during large storms.

Discussion

Performance Determination

Ongoing research determined that the flow rate sustained by the distribution pipe was limited by the orifices on the pipe wall, so the following analyses were based on the orifice flow equation. Assuming that partial clogging blocked a portion of orifice area, the orifice equation for a single orifice can be rewritten as Equation 1 shows. In Equation 1, q is the orifice flow rate, ϵ is the portion (ranging from 0 to 1) of orifice area that is functional, C is the orifice discharge coefficient, a is the orifice area before partial clogging happens, g is the gravity constant (9.8 m/s^2), and h_d is the pressure head driving the orifice flow (called “driving head” hereafter).

$$q = C(\epsilon a)\sqrt{2gh_d} \quad (1)$$

Equation 1 can be rearranged for p in Equation 2.

$$\epsilon = \frac{q}{Ca\sqrt{2gh_d}} = \frac{q}{(C\sqrt{2g})(a\sqrt{h_d})} \propto \frac{q}{a\sqrt{h_d}} \quad (2)$$

In Equation 2, C and g can be considered constants, so ϵ is linearly proportional to $\frac{q}{a\sqrt{h_d}}$. The authors decided to assume the discharge coefficient C as a constant, for the fact that the discharge coefficient C for parallel flow (i.e. flow in the pipe is parallel to the plane of the orifice) is in a narrow range of 0.61-0.64 [25].

For orifices uniformly distributed on a section of perforated pipe, Equation 2 can be rewritten as Equation 3 shows, where E is the mean portion of clogging on the section of pipe, Q is the sum of orifice flow generated by the section of pipe, A is the total orifice area on that section of pipe, n is the number of orifices on the section of pipe, $h_{d,i}$ represents the driving head at the i-th orifice, and $h_{d,mean}$ represents the mean driving head among all orifice on the section of pipe. The approximation performed in Equation 3 was permissible because the goal of derivation was to provide a means to compare relative magnitudes of partial clogging among different events.

$$\mathrm{E} \propto \frac{Q}{A\frac{\sum_{i=1}^{n}\sqrt{h_{d,i}}}{n}} \approx \frac{Q}{A\left(\sqrt{\frac{\sum_{i=1}^{n}h_{d,i}}{n}}\right)} = \frac{Q}{A\sqrt{h_{d,mean}}} \quad (3)$$

Since the orifices are uniformly distributed on the perforated pipe, the total orifice area on the section of pipe would be linearly proportional to the length of the pipe which allows orifice flow; therefore, a performance index i (Equation 4) can be derived to represent the performance of the perforated pipe based on Equation 3, with higher value representing less influence from partial clogging (i.e. higher performance).

$$i = \frac{Q}{l_{eff}\sqrt{h_{d,mean}}} \quad (4)$$

where l_{eff} is the effective length of distribution pipe that allows orifice flow, which is the equivalent length of water column with the same volume of water (V) in the pipe and the cross-sectional area (A) of the pipe, as explained by Equation 5.

$$l_{eff} = \frac{V}{A} \quad (5)$$

Detailed definitions of parameters (for $h_{d,mean}$ and l_{eff}) for the performance index under various scenarios were discussed below. *Figure 7* describes the operation of a typical distribution system. The datum is set at the elevation of the center of the distribution pipe at its inlet. Water elevation in the rock bed and in the inlet structure is z_R and z_{in}, respectively, with difference h_d. Along the centerline of the pipe (with inclination angle θ), the length of water (along the pipe centerline) above and below water in the rock bed (elevation z_R) is l_{above} ($\propto h_d$) and l_{below} ($\propto z_R$), respectively. For the condition

Preprints (www.preprints.org) | NOT PEER-REVIEWED | Posted: 4 July 2018 doi:10.20944/preprints201807.0075.v1

Peer-reviewed version available at Water 2018, 10, 1045; doi:10.3390/w10081045

considered by Figure 7, z_R and z_{in} are both lower than the top of the distribution pipe. Other conditions were analyzed as provided below.

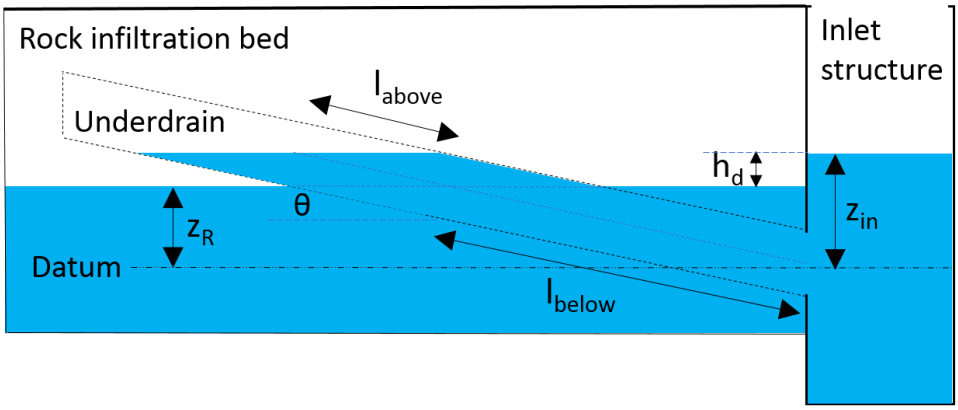

Figure 7. Profile view of a typical distribution system in this research

From recorded data, the water surface inside the distribution pipe and that in the inlet structure were very close to each other in elevation, as the difference of velocity head was proven to be negligible. It implied that the driving head was the water surface elevation difference h_d. The driving head was constant anywhere below the rock bed water surface z_R. The driving head above z_R was simply the hydrostatic pressure of the water column above z_R, with zero at the top of the water column and linearly increasing to h_d at the elevation of z_R. The mean driving head ($h_{d,mean}$) acting on the pipe can thus be derived in Equation 6 below.

$$h_{d,mean} \cong \left(\frac{h_d}{2} l_{above} + h_d l_{below}\right) \Big/ (l_{above} + l_{below})$$

$$= \left(\frac{{h_d}^2}{2} + h_d z_R\right) \Big/ z_{in} \quad (6)$$

The effective pipe length was simply provided by Equation 7:

$$l_{eff} \cong z_{in} \csc(\theta) \quad (7)$$

Other than the condition depicted by Figure 7, other four possible conditions were analyzed as Figure 8 illustrates. All items in Figure 8 were defined before except for h_{d1} and h_{d2}, indicating the distance from the water surface in the inlet structure to the top and the inlet of the distribution pipe (along its centerline) in Figure 8 (b), respectively. Note that conditions with either z_R or z_{in} below the top of the distribution pipe inlet were excluded from consideration because effective length of water in the pipe of such conditions cannot be based on the pipe length with fully wetted perimeter like that of other considered conditions.

Preprints (www.preprints.org) | NOT PEER-REVIEWED | Posted: 4 July 2018 doi:10.20944/preprints201807.0075.v1

Peer-reviewed version available at Water 2018, 10, 1045; doi:10.3390/w10081045

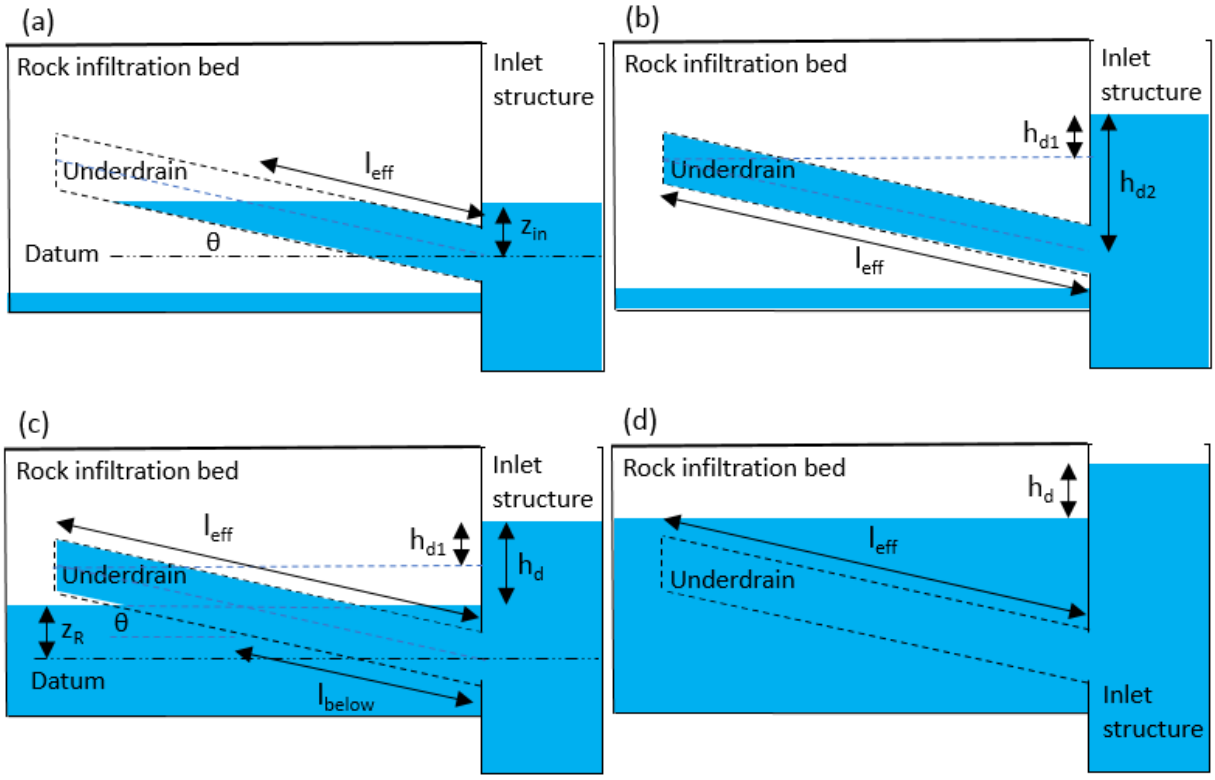

Figure 8. Conditiona considered in pipe performance determination in addition to the condition of Figure 7.

Analyses based on *Figure 8* (a) were similar to what has been done for the water column above z_R in *Figure 7*, with the mean driving head and the effective pipe length calculated by Equations 8 and 9 below:

$$h_{d,mean} \cong {}^{z_{in}}/_{2} \tag{8}$$

$$l_{eff} \cong z_{in}\csc(\theta) \tag{9}$$

Intense storms created conditions depicted by *Figure 8* (b), (c), and (d), in which the water elevation in the inlet structure builds up quickly. The distribution pipe was completely full, but water in the rock infiltration bed can still be relatively shallow. Similar to Equation 8, the mean driving head for *Figure 8* (b) was provided by Equation 10 below, and the effective pipe length l_{eff} is simply the length of the whole pipe.

$$h_{d,mean} \cong \frac{h_{d1}+h_{d2}}{2} \tag{10}$$

Figure 8 (c) has a form similar to that of *Figure 7* with the mean driving head for *Figure 8* (c) provided by Equations 11 below, while the effective pipe length (l_{eff}) is the length of the whole pipe (l_{pipe}).

$$h_{d,mean} \cong {}^{\left(\left(\frac{h_d+h_{d1}}{2}\right)\left(l_{pipe}-l_{below}\right)+h_d l_{below}\right)}/_{l_{pipe}} \tag{11}$$

where l_{below} is the length of pipe under z_R and is given by $l_{below} \cong z_R\csc(\theta)$.

Preprints (www.preprints.org) | NOT PEER-REVIEWED | Posted: 4 July 2018 doi:10.20944/preprints201807.0075.v1

Peer-reviewed version available at Water 2018, 10, 1045; doi:10.3390/w10081045

The last condition (Figure 8 (d)) had a constant driving head throughout the distribution pipe because the whole pipe is submerged, thus $h_{d,mean} = h_d$, and the effective pipe length l_{eff} is the length of the whole pipe l_{pipe}.

Performance Variations

Variations of orifice performance can be examined by plotting the measured flow rate against $l_{eff}\sqrt{h_{d,mean}}$, as shown by Figure 9 with data with zero flow excluded. All data from November 2016 to April 2018 is utilized in Figure 9. According to Equation 4, flow rate Q divided by $l_{eff}\sqrt{h_{d,mean}}$ in Figure 9 represents performance. The dates of partial clogging and no clogging were determined from Figure 4.

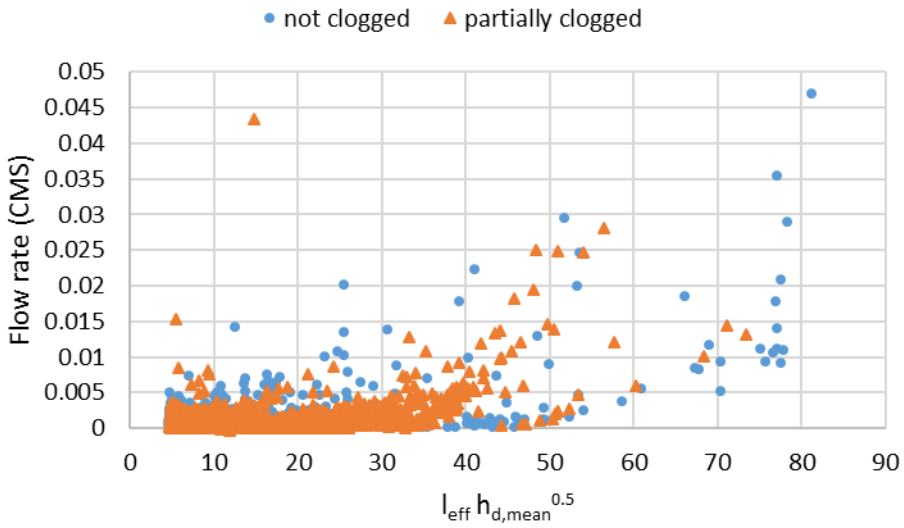

Figure 9. Performance plotted as flow rate vs. $h_{d,mean}l_{eff}$ for all data

$l_{eff}\sqrt{h_{d,mean}}$ appeared to be a strong predictor for flow rate with $p < 0.0001$ for both the non-clogging and partial clogging data. ANCOVA (ANalysis of COVAiance) was utilized to examine the effect of partial clogging on distribution pipe performance by adding one dummy variable of either 0 (represents no clogging) or 1 (represents partial clogging) in linear regressions. The result from ANCOVA showed strong evidence ($p < 0.0001$) that partial clogging had an impact on performance.

The above ANCOVA result was based on all data, with a large portion of data from periods with very slow drawdown of water level in the inlet structure after storms ended, as Figure 5 illustrates. Because the focus of this research was on how partial clogging can affect the orifice performance during larger storm events (when overflow occurs), the results from periods with slow drawdown and lower rainfall intensities were of less interest. Table 1 provides the ANCOVA results with different rainfall intensity criteria below which data entries were excluded. P-values showing no difference in performance between no clogging and partial clogging were in bold.

Preprints (www.preprints.org) | NOT PEER-REVIEWED | Posted: 4 July 2018 doi:10.20944/preprints201807.0075.v1

Peer-reviewed version available at Water 2018, 10, 1045; doi:10.3390/w10081045

Table 1. ANCOVA results with different rainfall intensity thresholds

Rainfall intensity criteria (mm/5 min)	0	0.2	0.4	0.6	0.65	0.7	0.8
Number of data points – no clogging	1259	477	320	223	213	208	194
Number of data points – partial clogging	3128	285	155	94	79	76	57
ANCOVA p-value	< 0.0001	< 0.0001	0.0002	0.0091	**0.061**	**0.098**	**0.826**

Table 1 shows that even though partial clogging has a significant effect during dry periods or low-intensity storms, its effect declines as the storm intensity increases. When rainfall intensity was higher than approximately 0.65 mm/5 minutes, the effect of partial clogging was not statistically distinguishable, and thus did not significantly impact system performance. The distribution of data with a rainfall intensity criterion of 0.65 mm/ 5 minutes was provided in *Figure 10* .

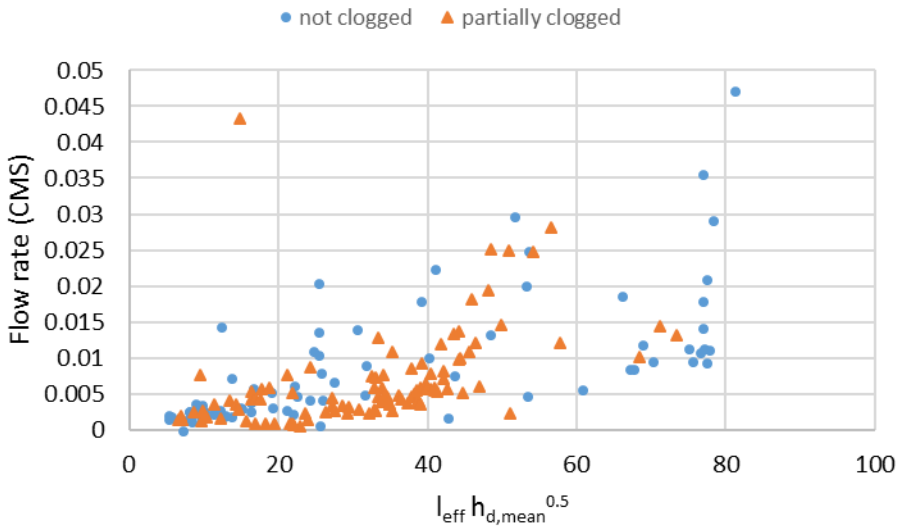

Figure 10. Performance plotted as flow rate vs. $h_{d,mean}l_{eff}$ for all data with 5-minute rainfall depth > 0.65 mm

Hypothesized Explanation

Firstly, drawdown data of the infiltration bed was examined. The relation between water depth and drawdown rate exhibited little variation throughout the observation period, thus showing no clogging of the infiltration bed. Therefore, the infiltration bed had no influence in explaining the results from the above analyses.

The record of subsurface maintenance done in the past was examined to explain the results from the analyses. The archived video observation (Jun 20, 2016) showed a significant quantity of debris deposited close to the 90-degree turn of the pipe near the entrance, as shown in Figure 11 (a). After passing the debris pile, the distribution pipe was generally clean as Figure 11 (b) shows. Another subsurface maintenance performed on Jan 25, 2017 found more debris, and the debris was piled mostly in the lower (i.e. close to the inlet) 30 meters of the pipe. The spatially uneven distribution of debris might be explained by the reversed slope of the distribution pipe that would bring most debris back to the entrance.

Peer-reviewed version available at Water 2018, 10, 1045; doi:10.3390/w10081045

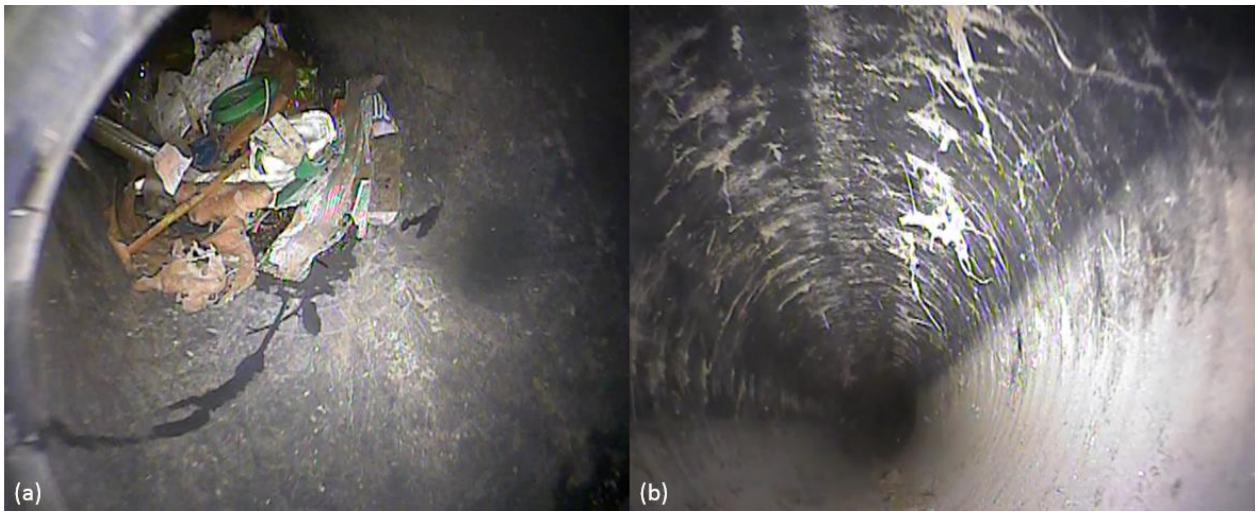

Figure 11. Images of debris deposition conditions before subsurface cleaning (Date: June 20, 2016).

Since most debris was accumulated near the lowest point of the distribution pipe, it appeared to cause partial clogging because water lower than the elevation of the debris cannot enter the rock infiltration bed through the orifices at the bottom section of the pipe. However, during storm events, the incoming water either moved the debris block thus exposing the orifices, or overtopped the debris block thus accessing the remaining distribution pipe. Such moving of debris can cause the partial clogging to break temporarily (e.g. Apr 10, 2017-Apr 17, 2017) as observed in Figure 4.

In Figure 11 (a), it is visible that a significant portion of debris appears to be leaves and paper with only a small portion being plastic, even though a trash guard has been installed in the inlet structure to minimize the amount of leaves entering the inlet structure with runoff. Due to the ample supply of fallen leaves in late autumn in Philadelphia, the debris pile would potentially continue to grow in winter if the leaves can get past the trash guard.

It was possible that as the supply of leaves stopped in winter and temperature started to increase in spring, the size of the debris pile dissipated through natural decomposition. No subsurface cleaning was performed after January 2017 in the observation period; therefore, natural decomposition was the only possible explanation. In any event, cleaning of the distribution pipe was recommended to reduce the amount of accumulated debris because the debris would not disappear completely and still cause short episodes of partial clogging during the summer. If left unchecked, the accumulated debris may block the distribution pipe and cause significant performance drop of the system.

Conclusion

Partial clogging of a distribution pipe system was found by both visual observations and data analyses as evidenced by continuous ponding in the inlet structure, partially submerging the entrance of the distribution pipe. The impact on orifice performance of the distribution pipe from such partial clogging was examined by plotting flow rate vs. $l_{eff}\sqrt{h_{d,mean}}$ where $h_{d,mean}$ is the mean driving head and l_{eff} the effective pipe length. ANCOVA was used to determine the impact of partial clogging on orifice

performance of the distribution pipe. Although partial clogging was found to exhibit a statistical significant effect on pipe performance, its effect declined with higher rainfall intensity, and eventually was not distinguishable when rainfall intensity was higher than approximately 0.65 mm/5 minutes. From an ongoing research, the system overflowed only when rainfall intensity was higher than approximately 3.3 mm/5 minutes. Therefore, partial clogging did not have any detrimental effect on overflow generating characteristics of this system.

Subsurface maintenance record showed that most debris was piled up near the lower portion of the distribution pipe, which caused the observed partial clogging. However, the incoming water during larger storms (rainfall intensity higher than approximately 0.65 mm/5 minutes) either moved the debris block thus exposing the orifices, or overtopped the debris block thus accessing the remaining distribution pipe, so the performance of the distribution system during larger storms was not affected. It was hypothesized that most debris was composed of leaves, which had abundant supply during late fall and early winter in Philadelphia. This explained why occurrence of partial clogging is the most frequent in winter.

Partial clogging was difficult to eliminate even with installation of a trash guard and regular cleaning of the distribution pipe. In Philadelphia or locations with similar climate and flora, a typical trash guard and regular (once to twice per year) pipe cleaning was sufficient to keep the distribution pipe system at satisfactory performance. It was suggested that future research interest can be focused on the following two directions; firstly, the minimal maintenance schedule needed to maintain the performance, and secondly, the relation between distribution pipe dimensions and the minimal needed maintenance schedule.

Acknowledgment

The support from Philadelphia Water Department is crucially important for the success of this study and is highly appreciated, particularly the assistance from Mr. Stephen White and Mr. Chris Bergerson. The assistance from Ms. Cara Albright (doctoral candidate of Villanova University) who designed and set up all instrumentation is also noted and highly appreciated.

This publication was developed under Assistance Agreement No. 83555601 awarded by the U.S. Environmental Protection Agency to Villanova University. It has not been formally reviewed by EPA. The views expressed in this document are solely those of Villanova University and do not necessarily reflect those of the Agency. EPA does not endorse any products or commercial services mentioned in this publication.

References

[1] Davis, A.P.; Hunt, W.F.; Traver, R.G.; Clar, M. Bioretention Technology: Overview of Current Practice and Future Needs. *J. Environ. Eng*. **2009**, *135(3)*, 109-117.

[2] Siriwardene, N.R.; Deletic, A.; Fletcher, T.D. Clogging of Stormwater Gravel Infiltration Systems and Filters: Insights from A Laboratory Study. *Water Research.* **2007**, *41(7)*, 1433-1440.

[3] Le Coustumer, S.; Fletcher, T.D.; Deletic, A.; Barraud, S.; Poelsma, P. The Influence of Design Parameters on Clogging of Stormwater Biofilters: A Large-Scale Column Study. *Water Research.* **2012**, *46(20)*, 6743-6752.

[4] Kandra, H.S.; McCarthy, D.; Fletcher, T.D.; Deletic, A. Assessment of Clogging Phenomena in Granular Filter Media Used for Stormwater Treatment. *J. Hydrology*. **2014**, *512*, 518-527.

[5] Pezzaniti, D.; Beecham, S.; Kandasamy, J. Influence of Clogging on The Effective Life of Permeable Pavements. *Water Management.* **2009**, *162*, 211-220.

[6] Lucke, T.; Beecham, S. Field Investigation of Clogging in A Permeable Pavement System. *Building Research & Information.* **2011**, *39(6)*, 603-615.

[7] Larrahondo, J.M.; Atalay, F.; McGillivray, A.V.; Mayne, P.W. Evaluation of Road Subsurface Drain Performance by Geophysical Methods. Proceedings of GeoCongress 2008: Geosustainability and Geohazard Mitigation, New Orleans, LA, U.S.A., March 9-12, 2008.

[8] Payne, E.; Hatt, B.; Deletic, A.; Dobbie, M.; McCarthy, D.; Chandrasena, G. *Adoption Guidelines for Stormwater Biofiltration Systems – Summary Report.* Cooperative Research Centre for Water Sensitive Cities, Clayton, VIC, Australia, 2015.

[9] Davis, A.P.; Traver, R.G.; Hunt, W.F.; Lee, R. Hydrologic Performance of Bioretention Storm-Water Control Measures. *J. Hydrol. Eng*. **2012**, *17(5)*, 604-614.

[10] Green City, Clean Waters. Available online: http://www.phillywatersheds.org/what_were_doing/documents_and_data/cso_long_term_control_plan (accessed on 6 April 2018).

[11] Murphy, P.; Kaye, N.B.; Khan, A.A. Hydraulic Performance of Aggregate Beds with Perforated Pipe Underdrains Flowing Full. *J. Irrig. Drain. Eng*. **2014**, *140(8)*, 04014023.

[12] Afrin, T.; Khan, A.A.; Kaye, N.B.; Testik, F.Y. Numerical Model for The Hydraulic Performance of Perforated Pipe Underdrains Surrounded by Loose Aggregate. *J. Hydraul. Eng.* **2016**, *142(8)*, 04016018.

[13] Ravina, I.; Paz, E.; Sofer, Z.; Marcu, A.; Shisha, A.; Sagi, G. Control of Emitter Clogging in Drip Irrigation with Reclaimed Wastewater. *Irrigation Science.* **1992**, *13(3)*, 129-139.

[14] Li, M.-H.; Barrett, M.E. Relationship Between Antecedent Dry Period and Highway Pollutant: Conceptual Models of Buildup and Removal Processes." *Water Environ. Res*. **2008**, *80(8)*, 740-747.

[15] Lee, J.H.; Bang, K.W. Characterization of Urban Stormwater Runoff. *Water Research.* **2000**, *34(6)*, 1773-1780.

[16] Grimm, N.B.; Faeth, S.H.; Golubiewski, N.E.; Redman, C.L.; Wu, J.; Bai, X.; Briggs, J.M. Global Change and The Ecology of Cities. *Science.* **2008**, *319 (5864)*, 756-760.

[17] Peel, M.C.; Finlayson, B.L.; McMahon, T.A. Updated World Map of The Koppen-Geiger Climate Classification. *Hydrology and Earth System Sciences.* **2007**, *11(5)*, 1633-1644.

[18] Climate Data Online. Available online: https://www.ncdc.noaa.gov/cdo-web/ (accessed on 6 April 2018).

[19] Products. Available online: https://www.campbellsci.com/products (accessed on 6 April 2018).

[20] Pyranometers & Solar Radiometers. Available online: http://www.huksefluxusa.com/products-services/solar-radiometers-pyranometers/ (accessed on 6 April 2018).

[21] User's Guide: Vaisala Weather Transmitter WXT520. Available online: https://www.vaisala.com/sites/default/files/documents/M210906EN-C.pdf (accessed on 6 April 2018).

[22] Featured Products. Available online: http://www.onsetcomp.com/ (accessed on 6 April 2018).

[23] Cloud Enabled Wireless Data Monitoring Systems. Available online: http://www.blue-siren.com/ (accessed on 6 April 2018).

[24] Soil Sensors. Available online: http://www.stevenswater.com/products/sensors/soil/ (accessed on 6 April 2018).

[25] Bailey, B.J. Fluid Flow in Perforated Pipes. *J. Mechanical Engineering Science.* **1975**, *17(6)*, 338-347.